Journal of Solid State Chemistry 182 (2009) 2769–2778

Contents lists available at ScienceDirect

Journal of Solid State Chemistry

journal homepage: www.elsevier.com/locate/jssc

Lanthanide N,N′-piperazine-bis(methylenephosphonates) (*Ln* = La, Ce, Nd) that display flexible frameworks, reversible hydration and cation exchange

John P.S. Mowat, John A. Groves, Michael T. Wharmby, Stuart R. Miller, Yang Li, Philip Lightfoot, Paul A. Wright *

School of Chemistry, University of St. Andrews, Purdie Building, North Haugh, St. Andrews, Fife KY16 9ST, UK

ARTICLE INFO

Article history:
Received 16 April 2009
Received in revised form
25 June 2009
Accepted 12 July 2009
Available online 18 July 2009

Keywords:
Phosphonates
Metal–organic frameworks
Cation exchange
Lanthanides

ABSTRACT

Hydrothermal syntheses of lanthanide bisphosphonate metal organic frameworks comprising the light lanthanides lanthanum, cerium and neodymium and N,N′-piperazine bis(methylenephosphonic acid) ($H_2L(1)$) and its 2-methyl and 2,5-dimethyl derivatives ($H_2L(2)$ and $H_2L(3)$) gives three new structure types. At elevated starting pH (ca. 5 and above) syntheses give 'type I' materials with all metals and acids of the study ($MLnLxH_2O$, M = Na, K, Cs; Ln = La, Ce, Nd; $x \approx 4$: $KCeL(1) \cdot 4H_2O$, $C2/c$, $a = 23.5864(2)$ Å, $b = 12.1186(2)$ Å, $c = 5.6613(2)$ Å, $\beta = 93.040(2)^\circ$). The framework of structure type I shows considerable flexibility as the ligand is changed, due mainly to rotation around the –N–CH_2– bond of the linker in response to steric considerations. Type I materials demonstrate cation exchange and dehydration and rehydration behaviour. Upon dehydration of $KCeL \cdot 4H_2O$, the space group changes to $P2_1/n$, $a = 21.8361(12)$ Å, $b = 9.3519(4)$ Å, $c = 5.5629(3)$ Å, $\beta = 96.560(4)^\circ$, as a result of a change of the piperazine ring from chair to boat configuration. When syntheses are performed at lower pH, two other structure types crystallise. With the 'non-methyl' ligand 1, type II materials result ($LnL(1)H_2L(1) \cdot 4.5H_2O$: Ln = La, $P\bar{1}$, $a = 5.7630(13)$ Å, $b = 10.213(2)$ Å, $c = 11.649(2)$ Å, $\alpha = 84.242(2)^\circ$, $\beta = 89.051(2)^\circ$, $\gamma = 82.876(2)^\circ$) in which one half of the ligands coordinate via the piperazine nitrogen atoms. With the 2-methyl ligand, structure type III crystallises ($LnHL(2) \cdot 4H_2O$: Ln = Nd, Ce, $P2_1/c$, $a = 5.7540(9)$ Å, $b = 14.1259(18)$ Å, $c = 21.156(5)$ Å, $\beta = 90.14(2)^\circ$) due to unfavourable steric interactions of the methyl group in structure type II.

1. Introduction

Metal organic frameworks are of much current interest as versatile and readily synthesised materials which exhibit adsorption, catalytic, magnetic and luminescent properties, depending on the metals included and the linking ligands. Carboxylates make up the most important class of these solids, including many members of the MOF (metal organic framework) and MIL (Material Institut Lavoisier) families prepared by the groups of Yaghi and Férey, respectively [1–4] and zeolitic imidazolate frameworks, ZIFs, have also become an important class of solid [5,6]. Metal phosphonate MOFs are less well represented, although the preparation and characterisation of porous pillared layered zirconium and titanium phosphonates is well documented [7,8]. There have been recent developments in the syntheses of 3D-connected microporous phosphonate frameworks [9,10] and N, N′-piperazine bis(methylenephosphonic acid) (Scheme 1, **1**) has been shown to be an effective linking ligand. The ligand shows versatile linking behaviour because the nitrogen atoms of the piperazine ring may or may not be protonated, and the bisphosphonate ligand itself can coordinate at each end through either two or three oxygen atoms and/or the ring nitrogen.

After the studies of the group of Zubieta on frameworks of **1** with vanadium and cobalt [11,12], the versatility of this ligand has been further demonstrated by the crystallisation of microporous (pore size ca. 10 Å) and three dimensionally connected coordination polymers based on divalent first row transition metals such as nickel and cobalt [13,14] and of the aluminium and titanium MIL-91 solids [15] that have small pores (ca. 4 Å). Lanthanide frameworks with **1** have also been prepared using lanthanum chloride as the metal source and the monohydrochloride derivative of the acid [16]. These have structures in which the chloride anions reside within the pores, directing the framework configuration by their hydrogen-bonding interactions. Lanthanide phosphonates and phosphonate-carboxylates themselves make up a growing class of solids, including open framework materials that display both porosity and luminescence, and are described in a comprehensive review by Mao [17] and more recent publications [18–21].

* Corresponding author.
E-mail address: paw2@st-and.ac.uk (P.A. Wright).

0022-4596/$ - see front matter © 2009 Elsevier Inc. All rights reserved.
doi:10.1016/j.jssc.2009.07.019

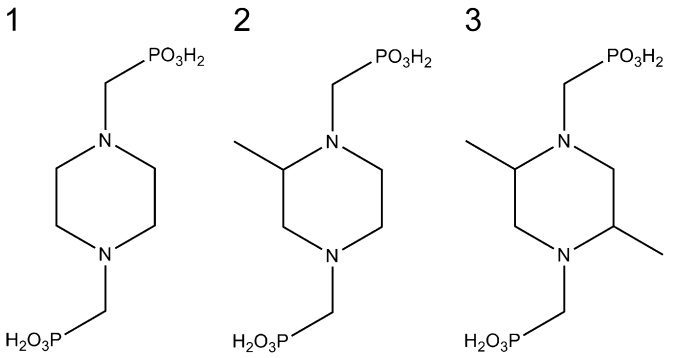

Scheme 1

We report here an investigation of the lanthanide phosphonate phases that are formed hydrothermally by the reaction of salts (other than chlorides) of the lighter and larger lanthanides (La^{3+}, Ce^{3+} and Nd^{3+}; 8-coordinate effective ionic radii 1.30, 1.28 and 1.25 Å, respectively) [22] with N,N′-piperazinebis(methylenephosphonic acid) **1** and its 2-methyl and 2, 5-dimethyl derivatives, **2** and **3** (Scheme 1). Exploratory studies at temperatures from 160 to 190 °C have given three new structure types for these lanthanides. Earlier studies have shown that gadolinium and yttrium bisphosphonates of **1** formed under similar conditions possess metal cations in octahedral coordination [18]. For the larger lanthanides La^{3+} to Nd^{3+}, the structures contain the lanthanides with higher coordination numbers (7 and 8). Furthermore, phase formation is found to be strongly influenced by the synthesis pH and by steric constraints imposed by the presence or absence of methyl groups on the piperazine ring. All the resulting framework solids display reversible water adsorption and the predominant solid formed at elevated pH exhibits a framework that shows cation exchange and a high degree of flexibility, depending on the ligand type used in its synthesis (**1**, **2** or **3**) and its degree of hydration.

2. Experimental

All ligands were synthesised using the modified Mannich reaction, following on from the published synthesis [16,18,23]. Details are given in the electronic supplementary information (ESI). Synthesis of the lanthanide phosphonates was performed by reacting selected metal salts and oxides of the representative lighter lanthanides La, Ce and Nd with bisphosphonic acids **1**, **2** and **3** under hydrothermal conditions in Teflon-lined autoclaves at temperatures from 160 to 190 °C. Prior to putting the reaction mixtures into the autoclave they were stirred at 80 °C for 1 h and in some cases the starting pH was modified by addition of a 0.1 M solution of alkali metal hydroxide (usually sodium or potassium, although cesium or alkylammonium hydroxides were also used successfully). Details of representative syntheses using phosphonic acids **1**, **2** and **3** are given in the ESI. The crystalline products were filtered, washed and dried. The solids were examined initially on a STOE STADI/P X-ray powder diffractometer, operating with monochromated Cu$K\alpha_1$ X-radiation ($\lambda = 1.54056$ Å), to identify the different phases and, in combination with single crystal and high resolution powder diffraction structure determination, their phase purity was established. Where possible, single crystal X-ray diffraction was performed. Additional structural information was derived from synchrotron X-ray powder diffraction, when single crystals could not be obtained, either at station ID-31, ESRF [24], or at station I-11, Diamond Light Source, Rutherford Appleton laboratory [25] (details in the ESI).

For phase pure samples, empirical formulae were determined by a measurement of the inorganic composition by EDX analysis on a JEOL 5680 SEM, elemental analysis of C, H and N and determination of water content by TGA, performed by heating in flowing air at 5 °C/min.

In order to determine the structural response to dehydration, selected samples of the different product phases were loaded into 0.7 mm quartz glass capillaries, attached to a gas handling line, and dehydrated under a vacuum of 10^{-4} Torr at a temperature of 160 °C, below that at which the framework was observed from the TGA to decompose. The capillary was then sealed and analysed by laboratory powder diffraction in Debye–Scherrer geometry. Subsequently, the capillary was broken open to allow re-adsorption of water from the atmosphere, and re-analysed by diffraction to determine whether the dehydration was reversible. For one material, which showed considerable change in the diffraction pattern upon dehydration, the pattern was collected using synchrotron powder X-ray diffraction of dehydrated solid in a sealed 0.7 mm quartz glass capillary at station ID-31, ESRF, as described above.

3. Crystallography

Tables in the Supplementary information give representative reactant ratios and crystallisation conditions, together with product phases, identified by numerals I–III according to the structure type and by the metals and ligand type present, for reactions of La^{3+}, Ce^{3+} and Nd^{3+}, with ligands **1**, **2** and **3**. Where the same structure type crystallises with different ligands, these are given the same Roman numeral, but with an associated number that relates to the ligand used (e.g. -II-**1**, -III-**3**, etc.). The framework-forming lanthanide and the (non-hydrogen) extra-framework cation content is also given (e.g. K,Ce-I-**1**). The phases were identified by their diffraction patterns, which were matched for the exactly corresponding materials by patterns simulated from the structures determined by single crystal diffraction to confirm phase purity (ESI). The presence of cations was established by EDX analysis. Within each structure type there are changes in the diffraction pattern depending on the ligand type used. Smaller differences in the position of diffraction maxima for the same structure type and ligand are observed when different lanthanide cations are present, due to their different sizes.

The structures K,Ce-I-**2**, La-II-**1** and Nd-III-**2** were solved from single crystal diffraction using the SHELX programme [26] and structures of K,Ce-I-**1**, dehydrated K,Ce-I-**1** and Na,Ce-I-**3** were obtained from refinement of structural models against synchrotron X-ray diffraction using the GSAS set of programmes [27]. Table 1 summarises the crystallographic parameters of materials examined by single crystal diffraction and Table 2 summarises the crystallographic data of samples studied by powder X-ray diffraction: the structures are described in the relevant sections below. Details of the crystallographic structure determination are given in the supplementary data.

4. Syntheses of phase I

Hydrothermal reactions of acid **1** with a variety of salts and oxides of the lanthanides La^{3+}, Ce^{3+} and Nd^{3+}, in which the initial pH is raised by addition of alkali metal hydroxides, give structure type I-**1** in microcrystalline form (Table 1, ESI). This was first identified from its characteristic powder diffraction pattern. Structures of type I-**1** crystallise from gels with starting pH values of 6.5 and above for La^{3+} and Ce^{3+}, and of 5 and above for Nd. At lower starting pH values other phases crystallise for La^{3+} and Ce^{3+},

Table 1
Details of the single crystal structure solutions of the representative examples of structure types I, II and III.

Product phase	K,Ce-I-**2**	La-II-**1**	Nd-III-**2**
Formula from chemical analysis	$K_{0.5}H_{0.5}CeL(\mathbf{2})\cdot 4H_2O$	$La_2L(\mathbf{1})H_2L(\mathbf{1})\cdot 4.5H_2O$	$NdHL(\mathbf{2})\cdot 4H_2O$
Asymmetric unit of structure solution	$K_{0.43}CeP_2O_6N_2C_6H_{12}\cdot 3.8H_2O$	$LaP_2O_6N_2C_6H_{13}\cdot 2.5H_2O$	$NdP_2O_6N_2C_7H_{15}\cdot 4H_2O$
Crystal system	monoclinic	triclinic	Monoclinic
Space group	$C2/c$	$P-1$	$P2_1/c$
a (Å)	23.144(9)	5.7630(13)	5.7540(9)
b (Å)	13.813(5)	10.213(2)	14.1259(18)
c (Å)	5.6241(19)	11.649(2)	21.156(5)
α (°)	90	84.242(2)	90
β (°)	102.251(17)	89.051(2)	90.14(2)
γ (°)	90	82.876(2)	90
V (Å^3)	1757.0(11)	676.9(2)	1719.6(5)
Z	4	2	4
ρ (g cm^{-3})	1.704	2.233	1.861
T (K)	113	93	113
Total/unique reflections	4621/1635	3987/2379	4655/1498
Reflections ($I>2\sigma(I)$)	1389	2168	1295
Parameters	88	174	148
Final R_1, wR_2($I>2\sigma(I)$)	0.093, 0.230	0.046, 0.124	0.090, 0.235

Table 2
Unit cell dimensions of materials with structure type I, with different lanthanide cation contents, (La, Ce, Nd) with different ligands (**1**, **2**, **3**) and also in the dehydrated state, as measured by laboratory and synchrotron powder X-ray diffraction.

	K,La-I-**1**	K,Ce-I-**1**	K,Nd-I-**1**	K,Ce-I-**1**	K,Ce-I-**2**	Na,Ce-I-**3**	K,Ce-I-**1** (dehydrated)
Diffractometer	Stoe	Stoe	Stoe	Synchrotron, ID-31	Synchrotron, ID-31	Synchrotron, I-11	Synchrotron, ID-31
λ of X-rays (Å)	1.54056	1.54056	1.54056	0.8002	0.8002	0.826019	0.8002
Temperature	RT	RT	RT	100 K	100 K	100 K	100 K
Crystal system	Monoclinic	Monoclinic	Monoclinic	Monoclinic	Monoclinic	Monoclinic	Monoclinic
Space group	$C2/c$	$C2/c$	$C2/c$	$C2/c$	$C2/c$	$C2/c$	$P2_1/n$
a (Å)	22.439(13)	22.560(16)	22.445(16)	22.5864(2)	23.0899(10)	22.9150(5)	21.8361(12)
b (Å)	11.942(9)	12.216(8)	12.165(12)	12.1186(2)	13.9954(8)	14.2802(3)	9.3519(4)
c (Å)	5.739(3)	5.648(5)	5.588(5)	5.6613(2)	5.6406(5)	5.6451(1)	5.5629(3)
α (°)	90	90	90	90	90	90	90
β (°)	91.76(3)	93.3(4)	92.88(5)	93.040(2)	102.5546(10)	102.8006(10)	96.560(4)
γ (°)	90	90	90	90	90	90	90
V (Å^3)	1537(2)	1554(3)	1524(4)	1547.42(5)	1780.06(7)	1801.36(5)	1128.56(11)

Nomenclature as described in the text.

but no crystalline product has yet been prepared with Nd^{3+} below pH 5. No crystals of suitable quality for SXRD were obtained using ligand **1.** EDX analysis indicates that phase I-**1** can incorporate alkali metal cations added during the synthesis.

Repeating the syntheses with bisphosphonic acid **2** with added alkali metal cations and initial pH values of 5–8 (for La^{3+}) and 7.5–8 (for Ce^{3+} and Nd^{3+}) gives type I materials (irrespective of the metal salt used) composed of small crystals that were studied by single crystal diffraction (Table 1). These materials have similar structures and composition to I-**1**, and give similar powder diffraction patterns, but with modified cell parameters. The single crystal structure of K–Ce-I-**2** is representative of this class of material. No single crystals of suitable quality for SXRD were obtained using ligand **3**, although the powder diffraction patterns of materials prepared using this ligand when alkali metal cations were added indicate materials of type I with good crystallinity. The unit cell parameters of K,Ce-I-**1**, K,Ce-I-**2** and Na,Ce-I-**3** obtained from synchrotron powder diffraction patterns collected at 100 K are compared in Table 2.

5. Structure type I $MLnL\cdot xH_2O$ (M = Na, K, Cs, H; Ln = La, Ce, Nd)

The structure of the cerium version of type I prepared with bisphosphonic acid **2** (K,Ce-I-**2**) as measured by single crystal diffraction is shown in Figs. 1a–c. Both potassium and cerium lie on two-fold axes. The framework consists of chains of edge-sharing CeO_8 polyhedra with distorted square anti-prism geometry, where all of the coordinating oxygen atoms belong to phosphonate groups of the ligand, so that all of the phosphonate oxygen atoms are bound to the lanthanide cations. Each 'metal phosphate' chain is linked to four other parallel chains via the bisphosphonate groups, the piperazine rings of which exhibit disorder over two different positions, each of which is in the chair configuration, with the methylene groups equatorial. For clarity, only one chair configuration is shown in Fig. 1a, without methyl groups. In type I structures prepared with phosphonic acid **2**, the methyl groups are not observed by diffraction (there are no significant peaks in the difference Fourier maps), and are thought to be disordered over all eight possible equatorial carbon positions of the piperazine rings. This arrangement of cerium phosphate chains and piperazine-based linkers gives channels in which alkali metal cations from the original synthesis (K^+ for the structure illustrated) and water molecules reside. In K,Ce-I-**2** the potassium ions are coordinated to phosphonate oxygen atoms around the cerium atoms, and water molecules are located bound to the potassium ions, between piperazine rings, and elsewhere in the channel. Crystallographic details of KCe-I-**2** are given in Table 1 and in the ESI. The same structure is adopted by lanthanum, cerium and neodymium forms of type I with ligand

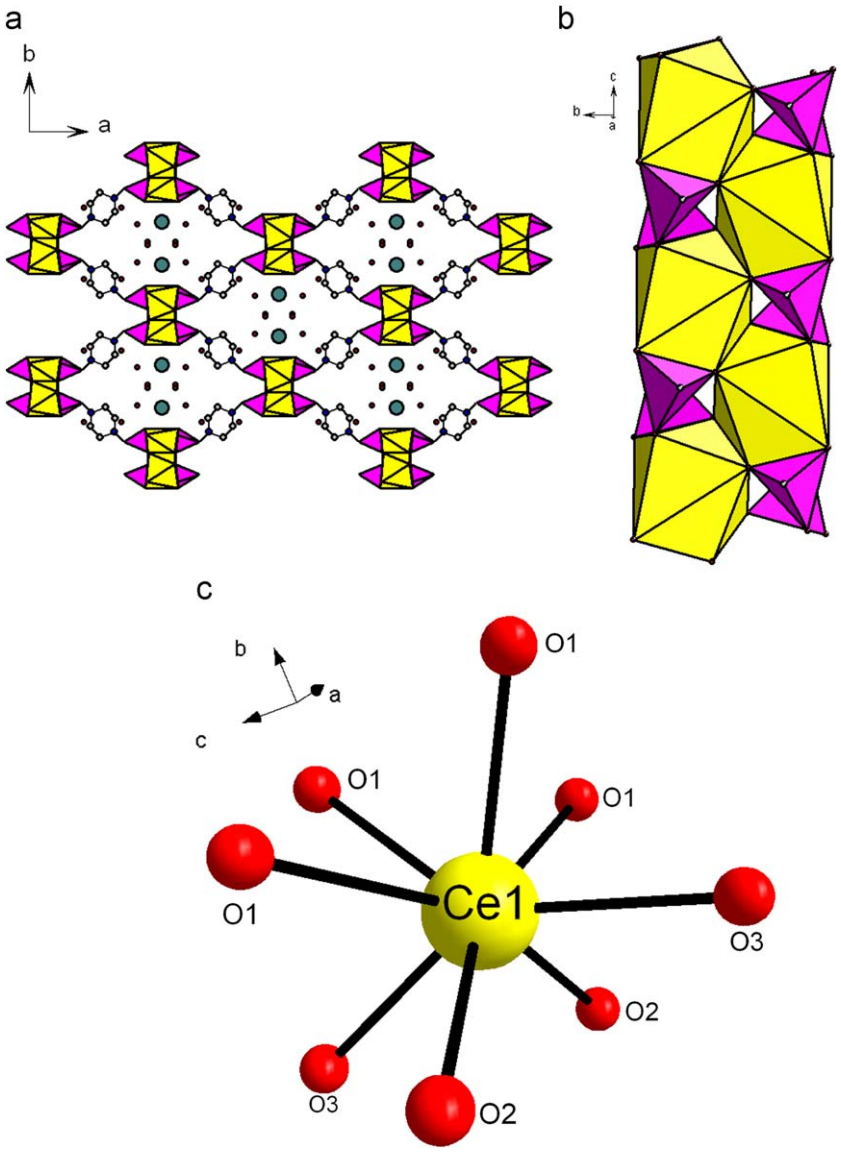

Fig. 1. (a) Structure of K,Ce-I-2 viewed down the channel axis; (b) the inorganic chain showing the lanthanide and phosphonate polyhedra; and (c) the CeO8 coordination environment. Lanthanide coordination polyhedra are depicted in yellow and the phosphonate tetrahedra in purple. Carbon and nitrogen atoms of the piperazine ring are shown as grey and smaller blue spheres, respectively, larger blue spheres depict the potassium cations and red spheres represent the oxygen atoms of physisorbed water molecules. (For interpretation of the references to color in this figure legend, the reader is referred to the web version of this article.)

2, using alkali metal hydroxides in the synthesis. For the La and Ce forms EDX confirms the presence of alkali metal cations in the final structure, but for Nd-I-**2** no alkali metal cations were observed, even though they were present in the synthesis and are required for crystallisation of this structure type. Charge balance in Nd-I-**2** is therefore attributed to protonated ligand.

As stated above, structures of type I are also prepared with phosphonic acids **1** and **3**, although only as microcrystalline powders. A comparison (Table 2) of the unit cell parameters at 100 K of cerium bisphosphonates with different phosphonic acids **1**, **2** and **3** indicates that the framework structure of type I is very flexible. A direct comparison of potassium cerium bisphosphonates prepared with ligands **1** and **2** in the hydrated form shows that the *b* axis length increases from 12.1186(2) Å to 13.9954(8) Å, the *a* axis length increases from 22.5864(2) Å to 23.0899(10) Å and β increases from 93.040(2)° to 102.5546(10)° when a methyl group is included in the ligand. This effect is also observed for Na,Ce-I-**3**, where the effect of adding a second methyl group on the ring leads to a further (smaller) change in the unit cell dimensions.

Figs. 2a–d compare the structures of K,Ce-I-**1** and Na,Ce-I-**3** viewed down the channel axis (a, b) and perpendicular to the cerium phosphate chains (c, d) and show the effect of the presence of two methyl groups on the piperazine rings on the structure. The equatorial plane of the rings lies approximately parallel to the channel axis in K,Ce-I-**1** and more nearly perpendicular to the channel axis in Na,Ce-I-**3**. This is thought to arise because the latter orientation results in the substituent methyl groups projecting into free space within the channels, whereas they would interact unfavourably with the cerium phosphate chains if the ring was in the former configuration. This rotation of the ring results in an opening of the lattice with a significant associated increase in the *b* axis length (17.8%).

Closer examination of the M,Ce-I structures reveals the structural mechanism by which these marked changes in unit cell dimensions occur. In all cases the piperazine ring is in the

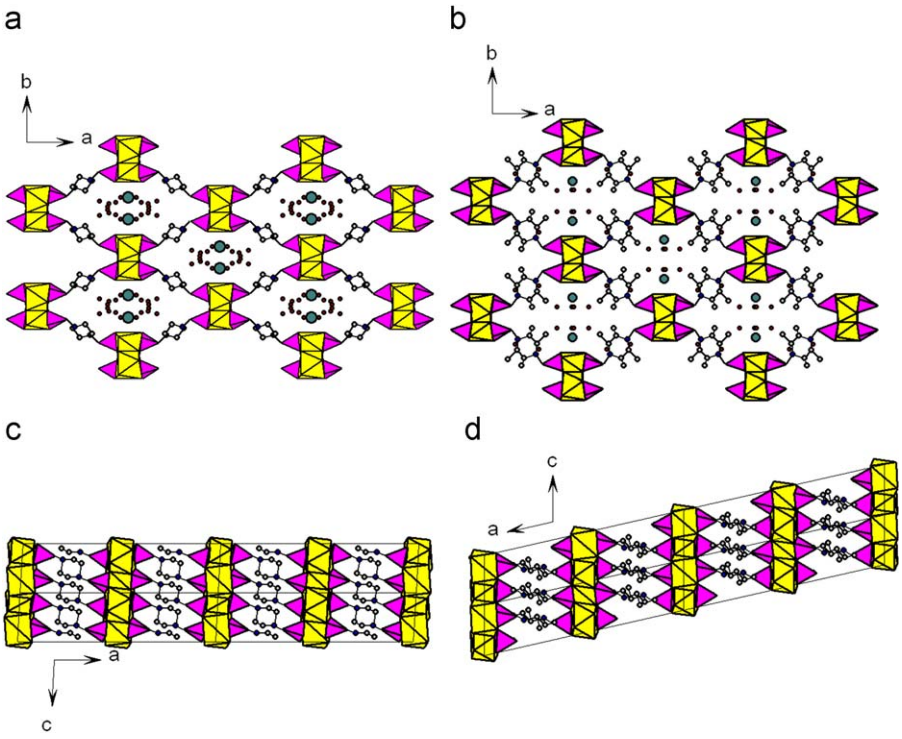

Fig. 2. Structures of Na–Ce-I-1 and K–Ce-I-3 viewed down the channel axis (a, b) and perpendicular to the inorganic chains (c, d) along [010]. Representation of atoms and coordination polyhedra as in Fig. 1. (For interpretation of the references to color in this figure legend, the reader is referred to the web version of this article.)

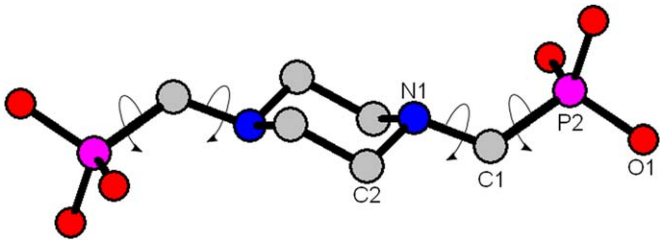

Fig. 3. Torsion angles around the C2–N1–C1–P2 and N1–C1–P2–O1 bonds of the ligand, shown here, strongly affect the structure. The values for different solids of structure type I are given in Table 3.

Table 3
Torsion angles in the N,N′-piperazine bis(methylenephosphonic acid) linker in type I structures K,Ce-I-**1** and Na,Ce-III-**3** (Geometries of the piperazine ring and phosphonate tetrahedron were strongly restrained).

	K,Ce-I-**1** (deg)	Na,Ce-III-**3** (deg)
C2–N1–C1–P2	78.136(4)	56.851(2)
N1–C1–P2–O1	177.984(4)	177.582(2)

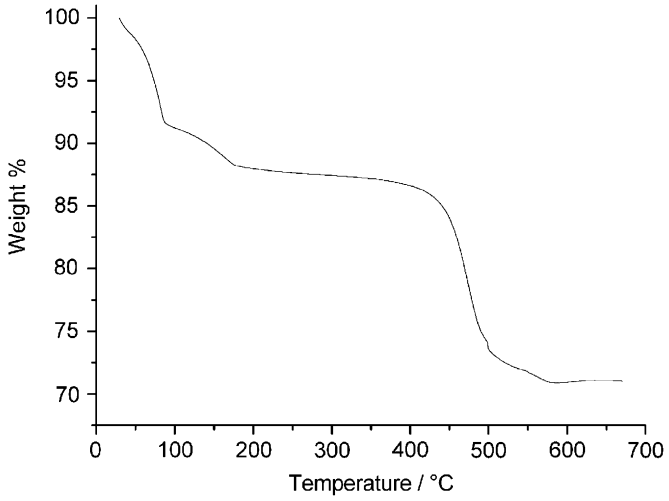

Fig. 4. TGA (flowing N2, heating rate 5 °C min^{-1}) of K,Ce-I-1.

chair configuration, so that most of the flexibility in the bisphosphonate ligand, and also in the structure, will derive from rotation about the N–C and C–P bonds. The torsion angles C2–N1–C1–P2 and N1–C1–P2–O1 (Fig. 3) for structures (K,H),Ce-I-**1** and Na,Ce-I-**3** are given in Table 3. This shows that it is the rotation about the N–C bond (of 21.3°) that is responsible for the structural change. (There is almost no rotation about N1–C1–P2–O1 (0.4°).)

Thermogravimetric analysis of structures of type I-**1** show two well defined weight loss events totalling 12–15% below 200 °C, attributed to water loss (as exemplified in Fig. 4 for K,Ce-I-**1**), and a further loss of 18–20 wt% starting at 400 °C, corresponding to loss of sample crystallinity as the ligand breaks down. The more strongly bound water (released above 90 °C) is attributed to molecules coordinated to the extra framework cations, the remainder being physisorbed water elsewhere in the pores. Similar thermal behaviour is observed for K,Ce-I-**2** and Na,Ce-I-**3**, although the two weight loss events are less well resolved in these materials.

Adsorption measurements on dehydrated K,Ce-I-**1** at 77 K indicate no microporosity for nitrogen adsorption up to 1 bar. The dehydration behaviour of phase I has been examined in more depth by synchrotron X-ray powder diffraction of dehydrated K,Ce-I-**1**. The structure undergoes a remarkable transformation to the dehydrated form (Figs. 5a–c). The piperazine ring changes to

the boat configuration and on one side of the ring the CH_2PO_3 group retains its equatorial position, while on the opposing N the CH_2PO_3 group adopts an axial position (Figs. 6a and b). The three phosphonate oxygen atoms on each end of the ligand remain coordinated to the lanthanide cation. The consequence of this rearrangement is that the *b* axis is greatly reduced in size as the channel is closed upon water loss and potassium ions remain coordinated to phosphonate oxygen atoms bound to the cerium. This explains the lack of porosity in the dehydrated solid. Upon exposing the dehydrated form to moist air, X-ray powder diffraction indicates that the dehydration is largely reversible, and the sample rehydrates to give a pattern similar to that of its as-prepared form (ESI).

The presence of extra-framework cations in type I materials suggested that they might possess ion exchange properties. Stirring suspensions of the as-prepared forms of *M*LnL-I in 0.1 M solutions of strontium or lanthanum nitrate at 70 °C for 2 h results in cation exchange of the sodium or potassium cations of the as-prepared forms with retention of crystallinity. According to EDX measurements on K,Nd-I-**1**, for example, 50% of the potassium is replaced by strontium and all of the potassium is replaced by lanthanum. According to X-ray diffraction, the materials remain crystalline during this ion exchange.

6. Structure types II and III

If the preparations are repeated with bisphosphonic acid **1** at 190 °C but without raising the initial pH from its original value of ca. 3 to more than 6, a second phase, II, is obtained for La^{3+} and Ce^{3+}, when starting with metal nitrates or acetates. Replacing ligand **1** with ligand **2** or **3** under lower initial pH conditions gives instead a third phase, III, for cerium and neodymium. This is shown in Scheme 2.

7. Structure type II $Ln_2L(\mathbf{1}) \cdot H_2L(\mathbf{1}) \cdot 4.5H_2O$ (Ln = La, Ce)

The structure of phase La-II-**1**, which forms in the absence of added alkali metal cations, is shown in Figs. 7a–c. Chains of edge-sharing 8-fold coordinated lanthanide coordination polyhedra running parallel to the *a* axis are linked to four other similar chains. In this structure, in contrast with phase I, the lanthanide coordination shells include seven phosphonate oxygen atoms and a nitrogen atom from the piperazine ring and there are two crystallographically and chemically distinct bisphosphonate linkers. Both have the piperazine ring in the chair conformation, with the N-methylene groups in equatorial positions. In one of the

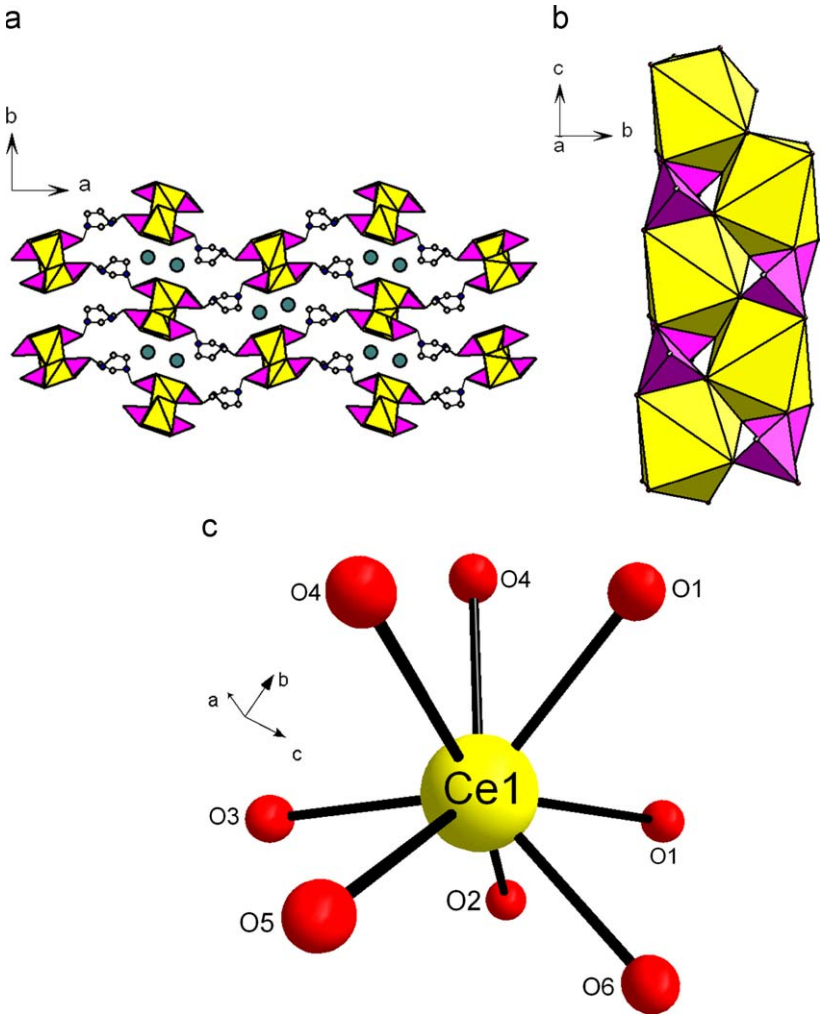

Fig. 5. (a) Structure of dehydrated K–Ce-I-1 viewed down the channel axis; (b) the inorganic chain showing the lanthanide polyhedra; and (c) the CeO_8 coordination environment. Representation of atoms and coordination polyhedra as in Fig. 1. (For interpretation of the references to color in this figure legend, the reader is referred to the web version of this article.)

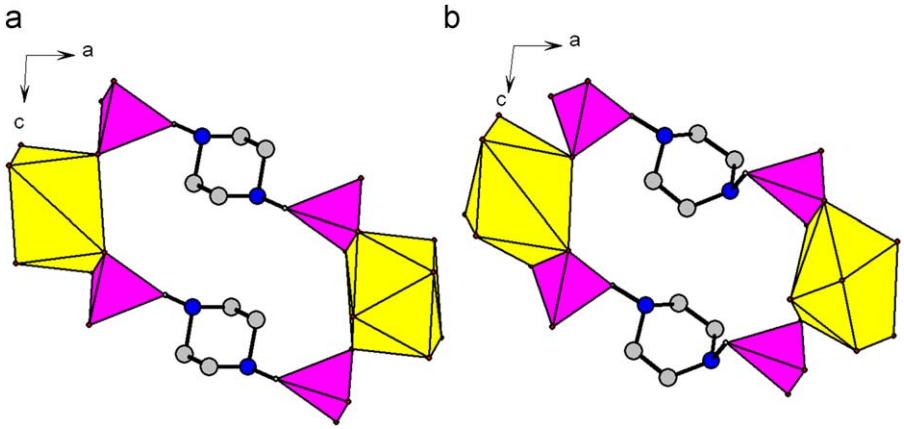

Fig. 6. Representations of part of the frameworks of K,Ce-I-1 in hydrated (a) and dehydrated (b) states, including two ligands bridging between lanthanide polyhedra in adjacent inorganic chains. The figures illustrate the change in configuration of the piperazine ring upon dehydration.

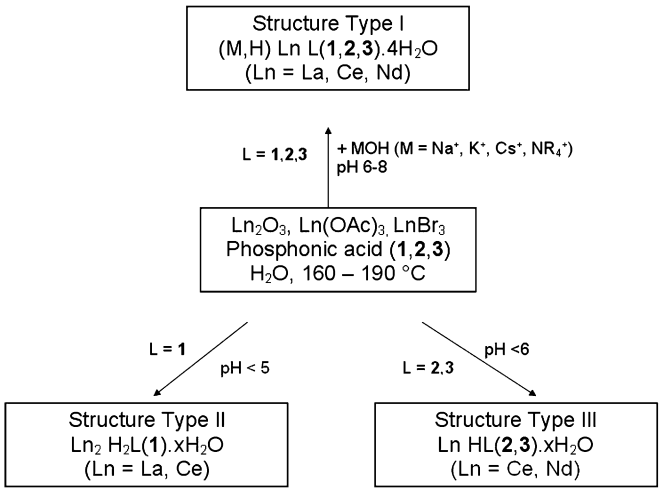

Scheme 2

linkers all six of the phosphonate oxygen atoms are coordinated to the lanthanum cation. The nitrogen atoms of this ligand are both protonated. The second linker has both nitrogen atoms and two out of the three phosphonate oxygen atoms of each phosphonate group coordinating to the lanthanum. The third oxygen atom on each phosphonate is assigned to a P = O group (P1–O3 = 1.53 Å) and undergoes H-bonding to N–H groups on the first ligand.

The lanthanide phosphonate chains are linked along *c* by ligands where all three oxygen atoms of each phosphonate group of the bisphosphonate ligand coordinate to lanthanide cations. The linkage along *b* is different, with bonding to the lanthanide cation from two phosphonate oxygen atoms and a ring nitrogen atom at each end of the ligand, leaving the third oxygen atom from the phosphonate unit H-bonded (O3–N2 = 2.531 Å) to a protonated nitrogen of the other bisphosphonate ligand. Water molecules reside within the small pores. Whereas in structure I-**1** the ligand is fully deprotonated and charge-balanced by alkali metal cations, in II-**1** one of the ligands is protonated and there are no cations. Thermal analysis shows that the water molecules (10 wt%) are lost below 100 °C, and that thermal decomposition occurs above 425 °C (ESI). No microporosity was measured for nitrogen at 77 K in the dehydrated sample but the sample readsorbs water from moist air.

8. Structure type III $Ln \cdot HL \cdot 4H_2O$ (Ln = Ce, Nd, $L = 2, 3$)

Structure type III as exemplified by NdHL(**2**) · $4H_2O$ is shown in Figs. 8a–c. The framework is built up from lanthanide phosphonate chains linked to four others by the bisphosphonate ligands, which are disordered over two chair configurations. These have the methylenephosphonate groups in equatorial positions, and there is some evidence for ordering of methyl groups at two positions on these rings. Each phosphonate oxygen atom is coordinated to a metal cation, so that the phosphonate PO_3C tetrahedra are corner-sharing with LnO_7 polyhedra.

Viewed down the channel axis this structure resembles structure type I, but inspection of the chains shows that there is no longer continuous Ln–O–Ln connectivity but instead the chain is made up of LnO_7 polyhedra (with Ln–O distances < 3 Å) linked along the chains by phosphonate groups. All except one of the coordinated oxygen atoms belongs to a phosphonate group, and the remaining coordinated oxygen is attributed to a water molecule. In the as-prepared, hydrated material, water occupies four other positions, two in the channels and two between the piperazine rings, where there are hydrogen bonds between the water oxygen and the ring nitrogen atoms, half of which are protonated to allow charge balance.

The distance across the pores from O(7), attributed to water coordinated to the neodymium cation, to hydrogen atoms linked to the ring carbon atoms, are small (4.5 Å) so that little space is available for adsorbates larger than water once the van der Waals radii of oxygen and hydrogen are accounted for. TGA indicates a weight loss of ca. 15% below 150 °C, attributed to the loss of adsorbed water (ESI). The structure retains crystallinity upon dehydration, but the higher angle diffraction peaks become broader as the long range order is decreased. The dehydrated structure does not adsorb nitrogen at 77 K.

9. Discussion

The hydrothermal reaction of salts and oxides of the light lanthanides La, Ce and Nd with the piperazine-based bisphosphonic acids of this study give three new structure types, in which the metal cations exhibit 7- or 8-fold coordination (Table 4). This contrasts strongly with previously reported materials based on the smaller gadolinium and yttrium cations, which show octahedral coordination [18]. The dominant structure type that is prepared at pH 6 and above for these lighter

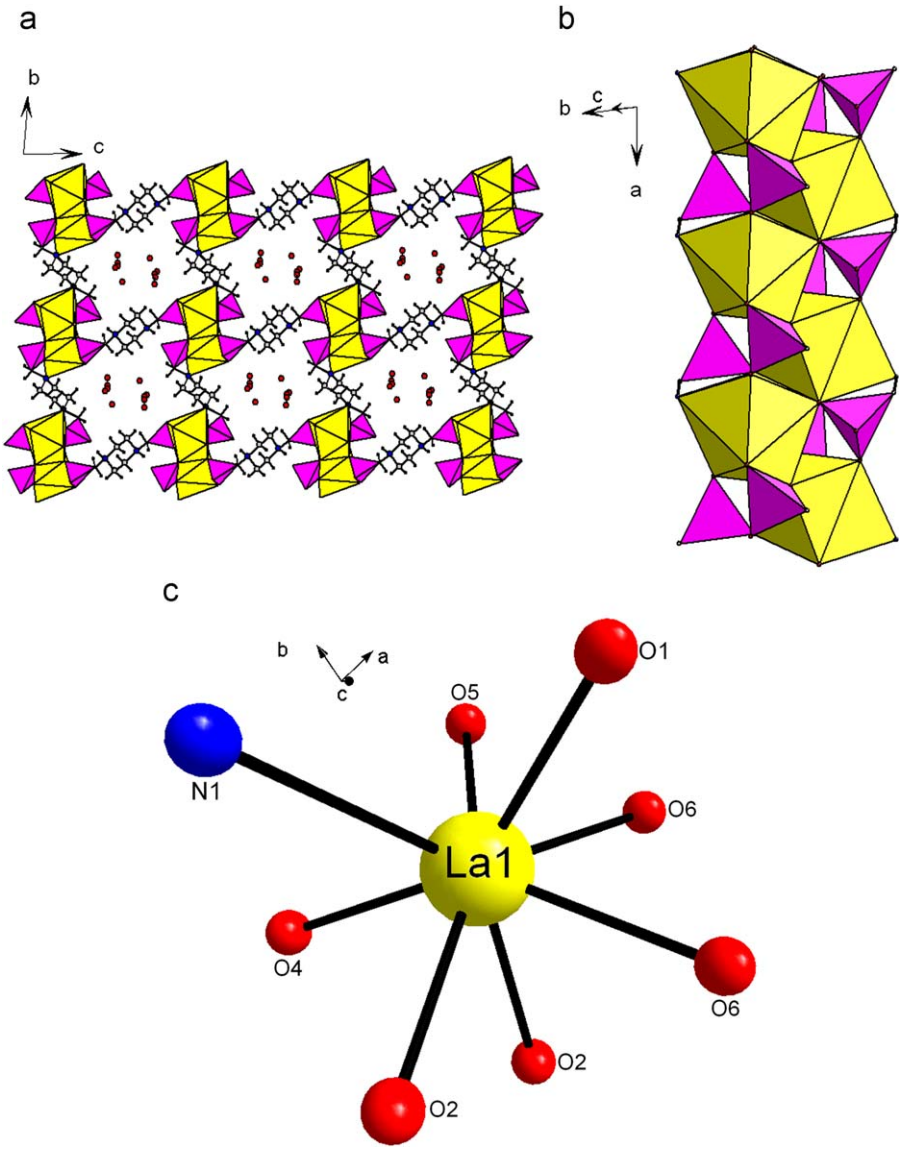

Fig. 7. (a) Structure of the La-II-1 viewed down the channel axis; (b) the inorganic chain showing the lanthanide polyhedra; and (c) the LaO_7N coordination environment. Representation of atoms and coordination polyhedra as in Fig. 1. (For interpretation of the references to color in this figure legend, the reader is referred to the web version of this article.)

(and larger) lanthanides is type I for all three ligands studied. This structure is a very flexible one, which is able to adapt to the presence or absence of one or two methyl group substituents on the piperazine ring by changes in the framework configuration. For the hydrated forms of the cerium-based solids, for example, the comparable unit cell dimensions are shown in Table 2. The largest change is observed along the *b* axis, which is associated with a scissoring motion of the lattice. As *b* increases, from 12.1 to 14.55 Å, the diamond shaped channel opens up to give more space for the additional methyl groups. At the same time, β increases from 96.56° to 102.8° as the angle that the bisphosphonate ligand makes with the lanthanide phosphonate chain is increased. This flexibility is possible in large part due to changes in torsion angles along the N–C and C–P bonds of the methylene phosphonate groups.

Upon dehydration the structure undergoes a large decrease in volume (37.3%) associated with a significant reduction in the *a* and *b* axes. The structural basis for this remarkable flexibility is the change of the ligand from chair to boat configuration. Once dehydrated the material exhibits no permanent porosity for gas adsorption. The dehydration is largely reversible, however.

There is more structural variety in the phases formed at lower pH than observed at the higher pH values. For bisphosphonic acid **1**, the structure type formed from syntheses with initial pH values of 4–6 is characterised by a framework structure in which one of the bisphosphonate units is coordinated to the lanthanides by two phosphonate oxygen atoms and one nitrogen of the ring, leaving a dangling P═O group H-bonded to the second ligand. The inorganic columns, like those in structure type I, are edge-sharing 8-coordinated lanthanide polyhedra, so the main chemical difference with that structure type is in the protonation of one of the ligands in structure type II. This is consistent with the difference in synthesis pH between the two phases.

Where ligands with methyl groups on the piperazine ring are present at low pH synthesis conditions, structure type II can no longer form because of steric hindrance (the methyl groups on the N-bonded ligands would be too close to oxygen atoms of the lanthanide chain). Instead, structure type III crystallises, in which the inorganic lanthanide phosphate columns consist of isolated

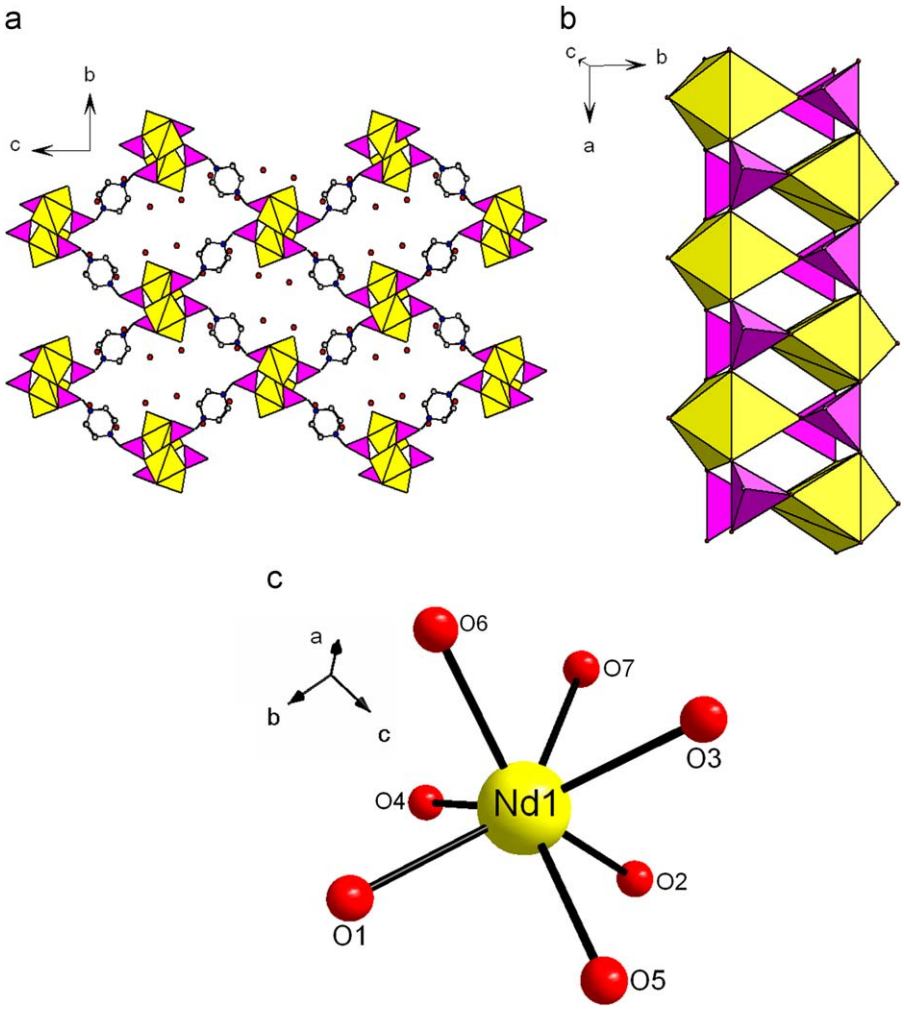

Fig. 8. (a) Structure of Nd-III-2 viewed down the channel axis (disordered methyl C atoms on the piperazine ring not shown); (b) the inorganic chain showing the lanthanide polyhedra; and (c) the NdO7 coordination environment. Representation of atoms and coordination polyhedra as in Fig. 1. (For interpretation of the references to color in this figure legend, the reader is referred to the web version of this article.)

Table 4
Table of bond distances (Å) for the lanthanide coordination, determined from single crystal diffraction or by refinement against synchrotron powder diffraction data.

K,Ce-I-**1**		KCe-I-**1** (dehydrated)		K,Ce-I-**2**		Na,Ce-III-**3**		K,La-II-**1**		K,Nd-III-**2**	
Ce1–O1	2.576(6)	Ce1–O1	2.346(5)	Ce1–O1	2.56(2)	Ce1–O1	2.527(12)	La1–O1	2.437(6)	Nd1–O1	2.373(14)
Ce1–O1	2.409(5)	Ce1–O1	2.811(15)	Ce1–O1	2.461(11)	Ce1–O1	2.445(14)	La1–O2	2.561(6)	Nd1–O2	2.388(17)
Ce1–O1	2.576(6)	Ce1–O2	2.673(15)	Ce1–O1	2.56(2)	Ce1–O1	2.527(12)	La1–O2	2.510(6)	Nd1–O3	2.409(17)
Ce1–O1	2.409(5)	Ce1–O3	2.381(17)	Ce1–O1	2.461(11)	Ce1–O1	2.445(14)	La1–O4	2.446(5)	Nd1–O4	2.34(2)
Ce1–O2	2.582(6)	Ce1–O4	2.544(18)	Ce1–O2	2.54(2)	Ce1–O2	2.395(12)	La1–O5	2.634(6)	Nd1–O5	2.381(11)
Ce1–O2	2.582(6)	Ce1–O4	2.315(18)	Ce1–O2	2.54(2)	Ce1–O2	2.395(12)	La1–O6	2.564(6)	Nd1–O6	2.35(2)
Ce1–O3	2.408(5)	Ce1–O5	2.52(2)	Ce1–O3	2.44(2)	Ce1–O3	2.345(13)	La1–O6	2.481(6)	Nd1–O7	2.611(17)
Ce1–O3	2.408(5)	Ce1–O6	2.34(2)	Ce1–O3	2.44(2)	Ce1–O3	2.345(13)	La1–N1	2.875(7)		

Nomenclature as described in the text.

LnO_7 polyhedra and all the ligands are protonated, consistent with the acidic conditions of their synthesis. Similar chains have previously been observed in two lanthanum-based structures with ligand **1** in the presence of chloride anions [16].

10. Conclusions

Bisphosphonate ligands based on the piperazine unit are shown to give a family of metal bisphosphonates frameworks for the early (larger) lanthanides La, Ce and Nd. The metal cations in these solids adopt seven or eight fold coordination with their coordination shell including phosphonate oxygen atoms, water molecules or even nitrogen atoms from the piperazine group. This is in contrast with smaller lanthanides, such as gadolinium or yttrium, which tend to favour six-fold coordination with ligand **1** under similar synthetic conditions. The materials display ion exchange properties and reversible dehydration.

Which structure type forms depends on a range of synthetic variables, including gel pH, anions from the metal salt used and

the presence or absence of methyl groups on the piperazine ring. The effect of varying pH is to determine the level of protonation of the ligand, which strongly affects its coordination and H-bonding behaviour. Synthesis in the presence of added alkali metal hydroxides results in deprotonated ligands and charge balancing cations in the pores, whereas lower pH synthesis leave protons on the ligand that readily form H-bonds either with uncoordinated P═O groups of the framework or with water molecules. The structural flexibility of the N,N′-piperazinebisphosphonate ligand enables it to crystallise successfully in a range of metal phosphonate MOFs. It may exhibit variable coordination (through nitrogen atoms and two or three oxygen atoms) depending on its state of protonation, the methylene phosphonate groups can be in equatorial or axial positions and the piperazine ring can exhibit either the chair or the boat configuration. Furthermore, the presence of methyl groups on the piperazine ring introduces steric factors and can thereby direct the crystallisation of different structures. Finally, in the current studies, the ligand is shown to be able to change configuration during dehydration, a process that is found to be reversible.

Supplementary information

Additional laboratory powder X-ray diffraction patterns, and synchrotron powder X-ray data, including Rietveld plots, as well as supplementary TGA traces, are given in the supplementary data, along with tables of synthetic conditions and product phases. Crystallographic information files are also included in the electronic supplementary information.

Acknowledgements

Dr. Irene Margiolaki (ESRF, Grenoble) and Drs. Chiu C. Tang, Steve Thompson and Julia Parker (Diamond Light Source, DLS) are thanked for help in collecting X-ray powder diffraction data. Part of this work was carried out with the support of the ESRF and the Diamond Light Source. The EPSRC (MTW, YL, PAW), the EC (SRM, DESANNS) and the University of St Andrews (JAG, JPSM, PL) are thanked for funding.

Appendix A. Supplementary material

Supplementary data associated with this article can be found in the online version at doi:10.1016/j.jssc.2009.07.019.

References

[1] H. Li, M. Eddaoudi, M. O'Keeffe, O.M. Yaghi, Nature 402 (1999) 276–279.
[2] O.M. Yaghi, M. O'Keeffe, N.W. Ockwig, H.K. Chae, M. Eddaoiudi, J. Kim, Nature 423 (2003) 705.
[3] G. Férey, C. Mellot-Draznieks, C. Serre, F. Millange, Acc. Chem. Res. 38 (2005) 217–225.
[4] G. Férey, Chem. Soc. Rev. 87 (2008) 191–214.
[5] X.C. Huang, Y.T. Lin, J.P. Zhang, X.M. Chen, Angew. Chem. Int. Ed. 45 (2006) 1557–1559.
[6] K.S. Park, Z. Ni, A.P. Côte, J.Y. Choi, R.D. Huang, F.J. Uribe-Romo, H.K. Chae, M. O'Keeffe, O.M. Yaghi, Proc. Natl. Acad. Sci. USA 103 (2006) 10186–10191.
[7] A. Clearfield, Z.K. Wang, Dalton Trans. (2002) 2937–2947.
[8] A. Clearfield, Curr. Opin. Solid State Mater. Sci. 6 (2002) 495.
[9] K. Maeda, Micropor. Mesopor. Mater. 73 (2004) 47–55.
[10] S.R. Miller, P.A. Wright, in: C.M. Lukehart, R.A. Scott (Eds.), Nanomaterials: Inorganic and Bioinorganic Perspectives, John Wiley & Sons, Ltd., Chichester, UK, 2008, pp. 659–672.
[11] V. Soghomonian, R. Diaz, R.C. Haushalter, C.J. O'Connor, J. Zubieta, J. Inorg. Chem. 34 (1995) 4460.
[12] R. La Duca, D. Rose, J.R. DeBord, R.C. Haushalter, C.J. O'Connor, J. Zubieta, J. Solid State Chem. 123 (1996) 408–412.
[13] J.A. Groves, S.R. Miller, S.J. Warrender, C. Mellot-Draznieks, P. Lightfoot, P.A. Wright, Chem. Commun. (2006) 3305–3307.
[14] S.R. Miller, G.M. Pearce, P.A. Wright, F. Bonino, S. Chavan, S. Bordiga, I. Margiolaki, N. Guillou, G. Férey, S. Bourrelly, P.L. Llewellyn, J. Am. Chem. Soc. 130 (2008) 15967–15981.
[15] C. Serre, J.A. Groves, P. Lightfoot, A.M.Z. Slawin, P.A. Wright, N. Stock, T. Bein, M. Haouas, F. Taulelle, G. Férey, Chem. Mater. 18 (2006) 1451–1457.
[16] J.A. Groves, P.A. Wright, P. Lightfoot, Inorg. Chem. 44 (2005) 1736–1739.
[17] J.G. Mao, Coord. Chem. Rev. 251 (2007) 1493.
[18] J.A. Groves, N.F. Stephens, P.A. Wright, P. Lightfoot, Solid State Sci. 8 (2006) 397–403.
[19] F.N. Shi, T. Trindade, J. Rocha, F.A.A. Paz, Cryst. Growth Des. 8 (2008) 3917–3920.
[20] F.N. Shi, L. Cunha-Silva, R.A.S. Ferreira, L. Mafra, T. Trindade, L.D. Carlos, F.A.A. Paz, J. Rocha, J. Am. Chem. Soc. 130 (2008) 150–167.
[21] Y.Q. Guo, S.-F. Tang, B.-P. Yang, J.-G. Mao, J. Solid State Chem. 181 (2008) 2713–2718.
[22] R.D. Shannon, C.T. Prewitt, Acta Cryst. B 25 (1969) 925–946.
[23] K. Moedritzer, R.R. Irani, J. Org. Chem. 31 (1996) 1603.
[24] A.N. Fitch, J. Res. NIST 109 (2004) 133–142.
[25] C.C. Tang, S.P. Thompson, T.P. Hill, G.R. Wilkin, U.H. Wagner, Z. Kristallogr. Suppl. 26 (2007) 153–158.
[26] G.M. Sheldrick, SHELX-97, University of Göttingen, Germany, 1997.
[27] A.C. Larson, R.B. von Dreele, Generalised Crystal Structure Analysis System, Los Alamos National Laboratory, USA, 1998.